International Journal of Electrical, Electronic and Communication Sciences
ISSN: 2517-9438
Vol:2, No:12, 2008

# Effect of Chromatic Dispersion on Optical Generation of Tunable Millimeter-Wave Signals

M. R. Salehi, S. Khosroabadi

***Abstract*****—** In this paper, the optical generation of three bands of continuously tunable millimeter-wave signals using an optical phase modulator (OPM) and a polarization state rotation filter (PSRF) as an optical notch filter is analyzed. The effect of the chromatic dispersion on millimeter-wave signals is presented.

***Keywords*****—** Optical generation, millimeter-wave, optical notch filter , chromatic dispersion.

## I. Introduction

FIBER-optic microwave and millimeter-wave links can be implemented by the use of direct detection techniques or remote heterodyne detection techniques [1]. In the direct detection-links, the millimeter-wave signal is intensity modulated onto the optical carrier from a laser. The optical signal is then transmitted through the optical fiber, and the millimeter-wave signal is recovered by direct detection in a photodiode. The fiber chromatic dispersion becomes a limiting factor for the transmission distance when the microwave signals are in the above 20 GHz regime. In order to cope with the limiting dispersion effects, optical self-heterodyne techniques as well as other remote heterodyne coherent schemes should be applied [2-4]. Several methods have been reported for the generation of modulated RF optical carriers in fiber-wireless systems. These include optical heterodyne and self-heterodyne techniques, and fundamental and harmonic signal generation using pulsed lasers [5-9].

Section II presents a system configuration that realizes a millimeter-wave signal generation system. In this section an extension to achieve a generating electrical signal is described. Section III shows the results. In this section, the spectrum of the generated electrical signals over the single mode fiber (SMF) is presented. The effect of the chromatic dispersion on the resulting signal is analyzed. A brief summary is given in Section IV.

M.R. Salehi is with Shiraz University of Technology, Shiraz, IRAN (corresponding author to provide phone: 98-711-7353500; fax: 98-711-7354514; e-mail: salehi@ sutech.ac.ir). This work is supported by the Shiraz Telecommunication Company in Iran (Grant No. 780 6021 9592).

S. Khosroabadi received the M.Sc. degree in electrical engineering from Shiraz University of Technology, Shiraz, IRAN (e-mail: s.khosroabadi@sutech.ac.ir).

## II. System Principle

The operating principle of the optical generation of millimeter-wave signals is illustrated in Fig.1.

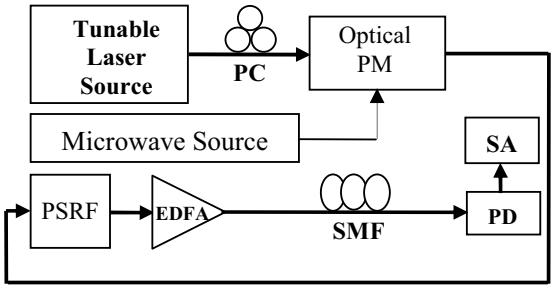


Fig. 1 Setup for optical generation of millimeter-wave signals. PD: Photodetector, PM: phase modulator, PC: polarization controller, EDFA: Erbium-doped fiber amplifier, SA: spectrum analyzer

The normalized amplitude of the phase-modulated optical field can be expanded in terms of Bessel functions of the first kind. The phase modulation process generates a series of sidebands with Bessel function amplitude coefficients. When the phase modulator is driven by an electrical signal with adequate power, a large value of the modulation depth ($\beta$) is obtained. In this case, the power in the input optical carrier will be spread out among the first-order, second-order, third-order, and higher order optical sidebands. The optical spectrum at the output of the phase modulator with different modulation depths is shown in Fig.2.

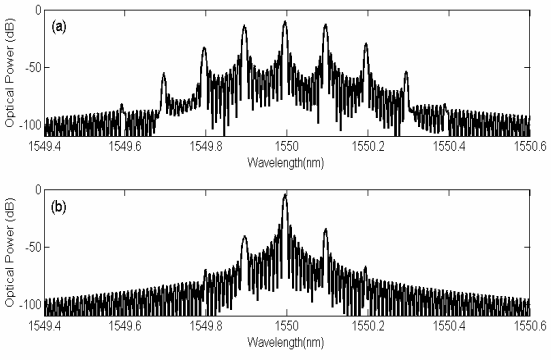


Fig. 2 Optical spectra with different modulation depths
(a) $\beta$ =1.4, (b) $\beta$ =0.3

In Fig. 2, $\beta=(\pi.V_{RF})/V_{\pi}$ is related to the phase-modulation depth, where $V_{\pi}$ is the half-wave voltage of the optical phase modulator and $V_{RF}$ is the amplitude of the electrical drive signal. In this figure, it is shown that when $\beta$ is small, only the first-order upper and lower sidebands can be considered, and higher-order sidebands are negligible. If $\beta$ is relatively large then the power levels of the higher order sidebands are comparable to those of the carrier and the first-order sidebands.

Fig.3 shows the Bessel function of the first kind of zero order as a function of modulation depth.

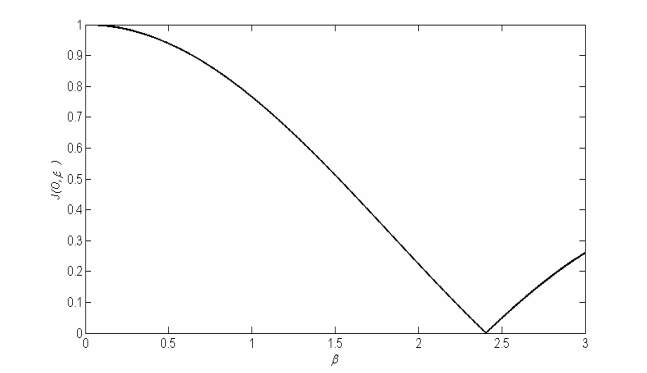


Fig.3 Bessel function of the first kind of zero order as a function of $\beta$.

In Fig.3, it is shown that the $J(0, \beta)$ is zero when the modulation depth is approximately 2.4. Therefore, we can obtain the amplitude of the RF signal $V_{RF}$ as

$$\beta = (\pi V_{RF}) / V_{\pi} = 2.4$$

Then

$$V_{RF} \cong 0.76 V_{\pi} \qquad (1)$$

The optical spectrum at the output of the phase modulator with different modulation depths is shown in Fig.4.

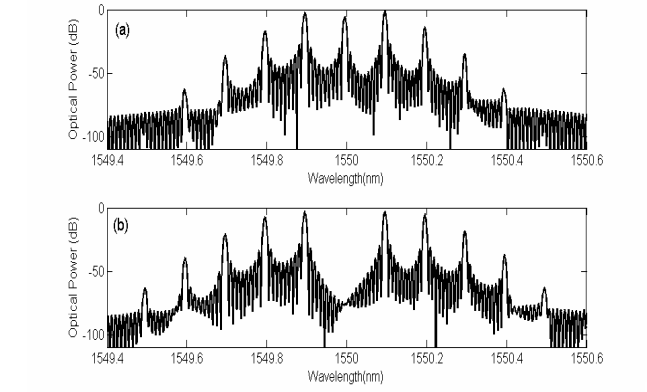


Fig.4 Optical spectra with different modulation depths
(a) $\beta$=1.8, (b) $\beta$=2.4

In Fig.4, it is shown that the optical carrier is completely suppressed corresponding to $\beta$=2.4.

The phase modulated signal after the PSRF can be written as

$$\begin{aligned} E_{out} = E_o\{&J_1\cos[(\omega_o+\omega_{RF})t+\frac{\pi}{2}]-\cos[(\omega_o-\omega_{RF})t-\frac{\pi}{2}] \\ &+J_2\cos[(\omega_o+2\omega_{RF})t+\pi]+\cos[(\omega_o-2\omega_{RF})t-\pi] \\ &+J_3\cos[(\omega_o+3\omega_{RF})t-\frac{\pi}{2}]-\cos[(\omega_o-3\omega_{RF})t+\frac{\pi}{2}] \\ &-J_o\cos(\omega_o t)\} \qquad (2) \end{aligned}$$

where $E_o$ and $\omega_o$ are the amplitude and angular frequency of the optical carrier. $\omega_{RF}$ is the modulating angular frequency of the electrical drive signal, and $J_n$ is the Bessel function of the first kind of order $n$.

The voltage expression of the generated electrical signals is

$$\begin{aligned} V_{out}(t) \cong AE_o^2[&J_1^2+J_2^2+J_3^2+J_1^2\cos(2\omega_{RF}t) \\ &+J_2^2\cos(4\omega_{RF}t)+J_3^2\cos(6\omega_{RF}t)] \qquad (3) \end{aligned}$$

where $A$ is a constant, which is related to $E_o$ and the responsivity of the PD. In this equation the limited bandwidth of the receiving circuit is also taken into account. Eq. (3) clearly indicates that there are no odd-order harmonic terms in the optically generated electrical signals once the carrier is removed and the proposed configuration is able to generate optically even-order harmonics of the electrical drive signal and suppress all odd-order harmonics.

## III. RESULTS

The optical carrier generated by the tunable laser source is sent to the phase modulator via a polarization controller. The optical spectra before and after the PSRF are shown in Fig. 5.

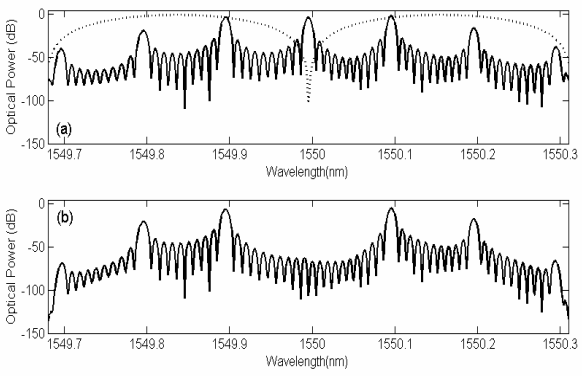


Fig.5 Typical optical spectra with β =1.6
(a) before the PSRF, (b) after the PSRF, (…) transfer function of PSRF with 24 ps group delay time.

Fig. 5 shows that optical sidebands are generated up to the fourth order. They are distributed symmetrically around the optical carrier. It is clearly shown in Fig. 5 that the optical carrier power is attenuated to higher than 40 dB. Fig. 6 shows the spectrum of the optically generated electrical signal without fiber chromatic dispersion at the output of the PD when the electrical drive signal is set to 8 and 10 GHz.

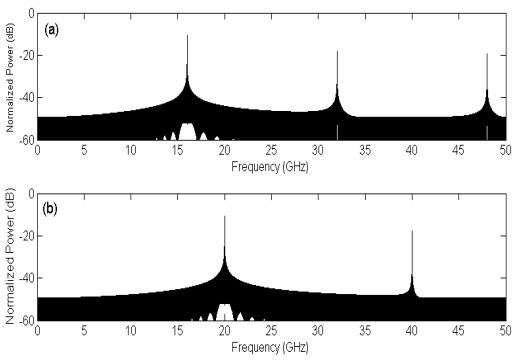


Fig.6 Spectrum of the generated millimeter-wave signals with the drive signal frequency (a)8 GHz , (b)10 GHz

It is seen that even-order frequencies of the drive electrical signal is generated. When the electrical drive signal is tuned from 8 to 10 GHz, three bands of millimeter-wave signals from 16 to 20 GHz, 32 to 40 GHz and 48 to 60 GHz with high frequency stability and narrow linewidth are generated. Although the chromatic dispersion of the SSMF is D =17 ps/(nm·km), it has to be considered when analyzing the quality of an electrical signal generated after the optical sidebands have traveled in a long fiber span. When fiber chromatic dispersion is taken into account, the propagation constant $\Omega(\omega)$ of the fiber for an optical sideband at $\omega_o \pm n\omega_{RF}$ can be approximately represented by a Taylor series around the center angular frequency $\omega_o$

$$\Omega(\omega_o \pm n\omega_{RF}) = \Omega(\omega_o) + \Omega'(\omega_o)(\pm n\omega_{RF}) + \frac{1}{2}\Omega''(\omega_o)(\pm n\omega_{RF})^2 + \cdots \quad (4)$$

The effect of higher order dispersion is neglected for the single-mode fiber at 1550-nm band and $\Omega''(\omega_o)$ can be expressed by the chromatic dispersion parameter $D$ as

$$\Omega''(\omega_o) = -\frac{c}{2\pi f_o^2} D \quad (5)$$

where $c$ is the speed of light in free space and $f_o$ is the frequency of the optical carrier. The voltage expression after the optical signal traveled through a fiber span of length $L$ and the electro-optical conversion can be written as

$$\begin{aligned} V_{out}(t) \cong AE_o^2\{&J_1^2 + J_2^2 + J_3^2 - [2J_2J_3 \times \sin(5\pi cDL(\frac{f_{RF}}{f_o})^2) \\ &+ 2J_1J_2 \times \sin(3\pi cDL(\frac{f_{RF}}{f_o})^2)] \times \cos(\omega_{RF}t - \omega_{RF}\Omega'(\omega_o)L) \\ &+ [J_1^2 - 2J_1J_2 \times \cos(8\pi cDL(\frac{f_{RF}}{f_o})^2)] \times \cos(2\omega_{RF}t \\ &- 2\omega_{RF}\Omega'(\omega_o)L) - [2J_1J_2 \times \sin(3\pi cDL(\frac{f_{RF}}{f_o})^2)] \\ &\times \cos(3\omega_{RF}t - 3\omega_{RF}\Omega'(\omega_o)L) + [J_2^2 - 2J_1J_3 \\ &\times \cos(8\pi cDL(\frac{f_{RF}}{f_o})^2)] \times \cos(4\omega_{RF}t - 4\omega_{RF}\Omega'(\omega_o)L) \\ &- [2J_2J_3 \times \sin(5\pi cDL(\frac{f_{RF}}{f_o})^2)] \times \cos(5\omega_{RF}t - 5\omega_{RF}\Omega'(\omega_o)L) \\ &+ J_3^2 \cos(6\omega_{RF}t - 6\omega_{RF}\Omega'(\omega_o)L)]\} \end{aligned} \quad (6)$$

where $f_{RF}$ is the frequency of the electrical drive signal. Fig.7 shows the spectra of the generated electrical signals over 25km length of the SSMF with 17 ps/(nm.km) chromatic dispersion parameter, when the microwave drive signal is tuned at 10 and 11 GHz.

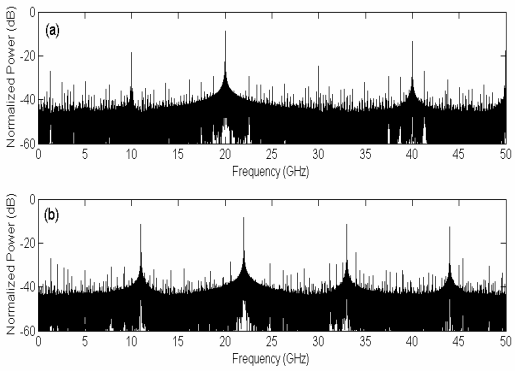


Fig.7 Spectrum of the generated millimeter-wave signals with the drive signal frequency (a) 10 GHz, (b) 11 GHz.

## IV. Conclusion

In this paper, the optical generation of wideband continuously tunable millimeter-wave signals is analyzed. When the generated optical sidebands were applied to a PD, only even-order electrical harmonics were generated. Three bands of millimeter-wave signals from 16 to 20 GHz, 32 to 40 GHz and 48 to 60 GHz were generated.

## References

[1] S. khosroabadi and M. R. Salehi, "Analysis of microwave photonic notch filter with tunable parameters," *IEEE Proc. Int. Conf. on Signal Processing*, Dobai, 2007, pp. 860-863.

[2] M. J. Wale, R. G. Walker, and C. Edge, "Single-sideband modulator in GaAs integrated optics for microwave frequency operation," *Integrated Photonics Research, OSA Tech. Dig. Ser,10*, 1992.
[3] A. Yariv, "Dynamic analysis of the semiconductor laser as a current-controlled oscillator in the optical phased-lock loop: applications," *Optics letters*, vol. *30*, pp. 2191-2193, 2005.
[4] L. A. Johansson and A. J. Seeds, "Generation and Transmission of Millimeter-Wave Data-Modulated Optical Signals Using an Optical Injection Phase-Lock Loop," *J. Lightwave Technol*, vol. *21*, 2003.
[5] T. Kuri and K. Kitayama, "Optical Heterodyne Detection Technique for Densely Multiplexed Millimeter-Wave-Band Radio-on-Fiber Systems," *J. Lightwave Technol*, vol. *21*, 2003.
[6] D. Eggemann, R. Bauer, S. Bornholdt, C. Mohrle, "Optical millimeter-wave generation and wireless data transmissionusing a dual-mode laser," *IEEE Photonics Technology Letters*, vol. *12*, pp. 1692–1694, 2000.
[7] J. Marti, J.M. Fuster, F. Ramos, "Optimization of millimeter-wave signal generation through FM-IM conversion in chirped fiber gratings," *Microwave and Optical Technology Letters, 27*, pp. 393–395, 2000.
[8] D. Kim, M. Pelusi, Z. Ahmed, D. Novak, H.-F. Liu, and Y. Ogawa, "Ultra stable millimeter-wave signal generation using hybrid mode locking of a monolithic DBR laser," *Electron. Let.*, *31*, pp. 733–734, 1995.
[9] X. Yu, H. Zhang, X. Zheng, "High carrier suppression double sideband modulation using polarization state rotation filter and optical external modulator," *Optics Communications*, *267*, pp. 83–87, 2006.